



CHORUS

This is the accepted manuscript made available via CHORUS. The article has been published as:

Parameterization dependence of T-matrix poles and eigenphases from a fit to πN elastic scattering data

R. L. Workman, R. A. Arndt, W. J. Briscoe, M. W. Paris, and I. I. Strakovsky

Phys. Rev. C **86**, 035202 — Published 7 September 2012

DOI: [10.1103/PhysRevC.86.035202](https://doi.org/10.1103/PhysRevC.86.035202)

Parameterization Dependence of T -matrix Poles and Eigenphases from a Fit to πN Elastic Scattering Data

R. L. Workman,¹ R. A. Arndt*,¹ W. J. Briscoe,¹ M. W. Paris^{†,1} and I. I. Strakovsky¹

¹*Data Analysis Center at the Institute for Nuclear Studies, Department of Physics, The George Washington University, Washington, D.C. 20052*

We have studied the form-dependence of fits to πN elastic scattering data, based on a Chew-Mandelstam K -matrix formalism. Extracted partial-wave amplitudes, and resonances characterized by T -matrix poles, are compared in fits generated with and without explicit Chew-Mandelstam K -matrix poles. Diagonalization of the S -matrix yields the eigenphase representation. While the eigenphases can vary significantly for the different parameterizations, the locations of most T -matrix poles are relatively stable. We also find the partial-wave amplitudes for πN elastic scattering to be quite stable. By turning the on and off the explicit Chew-Mandelstam pole contributions, we are able to determine how the T -matrix poles are generated in this approach.

PACS numbers: PACS numbers: 11.55.Bq, 11.80.Et, 11.80.Gw

I. INTRODUCTION

The excited states of the nucleon [1] have been studied in a wide array of reactions initiated mainly by pion and photon beams. Other approaches have involved an examination of the invariant mass distribution of products from, for example, nucleon-nucleon reactions [2] and J/Ψ decays [3]. Most non-strange states listed by the PDG [1] were identified from fits to πN elastic scattering and reaction data. Photo-decay amplitudes were determined mostly through analyses of single-pion photoproduction data.

Recent measurements of cross section and polarization quantities, related to the photo- and electroproduction of states other than πN , have been analyzed separately and in multi-channel approaches. These studies have provided stronger evidence for states seen only weakly in πN elastic scattering, and have suggested new states, coupling more strongly to other channels [4].

Among the most extensive πN scattering analyses [5–7], the parametrization of Ref. [7] based on the SAID interactive fitting and database codes [8] (the SAID-GW fit), utilizing the most recent data, has found the fewest number of N and Δ resonances. In the fit of Ref. [9], a search for weaker structures was carried out. There, the existing solution was modified using a simple product S -matrix approach, to include the effect of an added Breit-Wigner resonance in each partial wave. Chi-squared was mapped for various combinations of masses, widths and branching fraction. Two marginally significant candidates were found in the S_{11} and F_{15} partial waves, with pole positions: $1689 - i96$ MeV (for S_{11}) and $1793 - i94$ (for F_{15}). Of these, the F_{15} has been reported in subsequent fits, while the S_{11} has not.

tailed further below, existing GW-SAID fits to πN elastic scattering data have utilized a fit form based on the Chew-Mandelstam (CM) K -matrix. This approach is capable of generating T -matrix poles without the assumption of explicit CM K -matrix poles. Previous fits [7] have only included an explicit CM K -matrix pole for the $\Delta(1232)$. In the present study, an alternative parametrization with one explicit CM K -matrix pole in each partial wave was used to generate a fit independent of the usual CM parametrization.

A third form, based on a product S -matrix, constructed from pieces containing either CM K -matrix pole or non-pole terms, was also attempted. There, the goal was a separation of resonant and non-resonant contributions. Ultimately, this was not successful. As a result, we detail only the second approach, but comment on the product form in our conclusions.

The motivation for these new fits is twofold. By changing the parameterization, we are able to gauge the stability of the amplitudes and resonance positions. We are also able to see if the addition of new explicit CM K -matrix poles translates into additional resonance signals. Each fit was fully constrained by forward and fixed- t dispersion relations, and extrapolated into the complex energy plane to find T -matrix poles. As a result, this project constitutes the most extensive analysis of πN elastic scattering data since our first incorporation of dispersion relation constraints.

Below, in Sec. II, we briefly review the CM K -matrix formalism used in this and previous fits. The eigenphase representation, and some numerical details, are reviewed in Sec. III. Results for the partial wave fits and resonance spectrum are compared in Sec. IV. Finally, in Sec. V, we consider the implications of this and future work.

II. CHEW-MANDELSTAM FORMALISM

The Chew-Mandelstam (CM) approach, for the parametrization of multichannel hadronic πN elastic

*Deceased

[†]Current address: Theory Division, Los Alamos National Laboratory, Los Alamos, NM 87545, USA

Here we have considered another approach. As de-

scattering and reactions to other hadronic channels, has been described in detail in Refs. [7, 9–12]. The χ^2 -fits to data have been additionally constrained using the forward C^\pm dispersion relations and fixed- t dispersion relations for the invariant B amplitudes.

As a point of reference, we note that the standard CM parametrization can be expressed in terms of the on-shell Heitler partial wave K -matrix, K as

$$K^{-1}(E) = \overline{K}^{-1}(E) - \text{Re}C(E), \quad (1)$$

where E is the (complex) scattering energy, \overline{K} is the CM K -matrix and C is a diagonal matrix, whose matrix elements are termed the CM functions [13]. The Heitler K -matrix is related to the partial wave transition amplitude matrix, T as

$$T^{-1}(E) = K^{-1}(E) - i\rho(E). \quad (2)$$

Here, $\rho(E) = \delta(E - H_0)$, where H_0 is the (model independent) relativistic free-particle Hamiltonian with physical (stable) particle masses. It determines the CM functions, $C(E)$ via the relation $\text{Im}C(E) = \rho(E)$.¹

The standard form used in the GW fits is defined by the choice for the CM K -matrix elements

$$\overline{K}(E) = \sum_n c_n \overline{z}^n(E), \quad (3)$$

where c_n are a set of constants and \overline{z} is a linear function of the scattering energy, E . The integer, n is typically between 2 and 5, and depends on the matrix element in question.

Note that \overline{K} defines an entire function of the complex parameter E for finite values. This form is used for all but the P_{33} partial wave, which includes an explicit pole in \overline{K} . For partial waves other than the P_{33} , we see that the CM K -matrix, \overline{K} , is without poles (or other singularities). The Heitler K -matrix, K ,

$$K = \frac{1}{1 - \overline{K}[\text{Re}C]} \overline{K} \quad (4)$$

has a pole whenever $\det[1 - \text{Re}C(E)\overline{K}(E)] = 0$. The matrices K and \overline{K} are free of branch point singularities [12, 14].

The alternate form of the CM K -matrix is similar to the form used in the P_{33} partial wave of the standard \overline{K} parametrization, described above. This form is given by

$$\overline{K}_{ij} = \frac{\gamma_i \gamma_j}{E - E_p} + \beta(E)_{ij}. \quad (5)$$

Here, $\gamma_i(E)$ is a polynomial without a zero at the pole position, E_p , and the index labels the channel (πN , $\pi\Delta$, ρN , and ηN), $\beta(E)$ is an entire function of the complex energy, E .

III. EIGENPHASE REPRESENTATION

The fit produces a unitary S -matrix of amplitudes for all contributing channels. While those channels not fitted to data are unlikely to give a quantitative representation of the reaction (for example, $\pi N \rightarrow \pi\Delta$), they can be used to construct a set of eigenphases, which provide an interesting characterization of resonance behavior.

The unitarity of the S -matrix implies that its eigenvalues are phase factors. The matrix, U , of eigenvectors diagonalizes the S -matrix as

$$U^\dagger S U = \lambda, \quad (6)$$

where

$$\lambda = \begin{pmatrix} \lambda_1 & 0 & \cdots & 0 \\ 0 & \lambda_2 & \cdots & 0 \\ 0 & 0 & \ddots & 0 \\ 0 & 0 & \cdots & \lambda_n \end{pmatrix}. \quad (7)$$

Exploiting $|\lambda_i| = 1$, we write

$$\lambda_i = e^{2i\phi_i} \quad (8)$$

with ϕ_i real.

Our objective is the numerical evaluation of the eigenphases given the T -matrix elements from various fits. This is straightforward at a given energy, using a standard routine to diagonalize the unitary S -matrix. The only complicating issue is correlating a given eigenphase, $\phi_i(E)$ with the appropriate eigenchannel when two (or more) eigenphases converge as the energy changes. In other words, once an eigenchannel i is determined, we must track it for all energies. The no-crossing theorem [15] is readily generalized to unitary matrices and shows that, in a given partial wave, the eigenphases may not be equal for any energy. This property is exhibited in the eigenphase plots discussed below.

Given the T -matrix at some energy, $T(E)$, we can form the $S(E)$ -matrix. We diagonalize this matrix using a standard routine to obtain the eigenvalues $\{\lambda_i(E)\}_{i=1}^n$, where n is the number of channels.

If the eigenvalues are nearly degenerate at some energy, it is difficult to distinguish which eigenvalue corresponds to a given eigenchannel, say i , since diagonalization of S doesn't preserve the eigenchannel ordering. The set of eigenvectors, however, must be orthogonal at any energy; and, for continuous partial wave amplitudes, the change of the eigenvector for a given eigenchannel is small for nearby energies.

The eigenchannels are maintained using the following method. The S -matrix is diagonalized at the initial energy, say $E_1 = 1150$ MeV. We obtain n eigenphases (where n is the number of channels included for the given partial wave), $\lambda_1(E_1), \dots, \lambda_n(E_1)$ and their corresponding eigenvectors $v_1(E_1), \dots, v_n(E_1)$. We wish to correlate the eigenvalues and eigenvectors with a given eigenchannel throughout the evaluation of the eigenvalues at higher energies, $E > E_1$.

¹ The included quasi-two-body channels, such as $\pi\Delta$, are constrained by a subtracted dispersion relation to be zero at the stable three-body threshold.

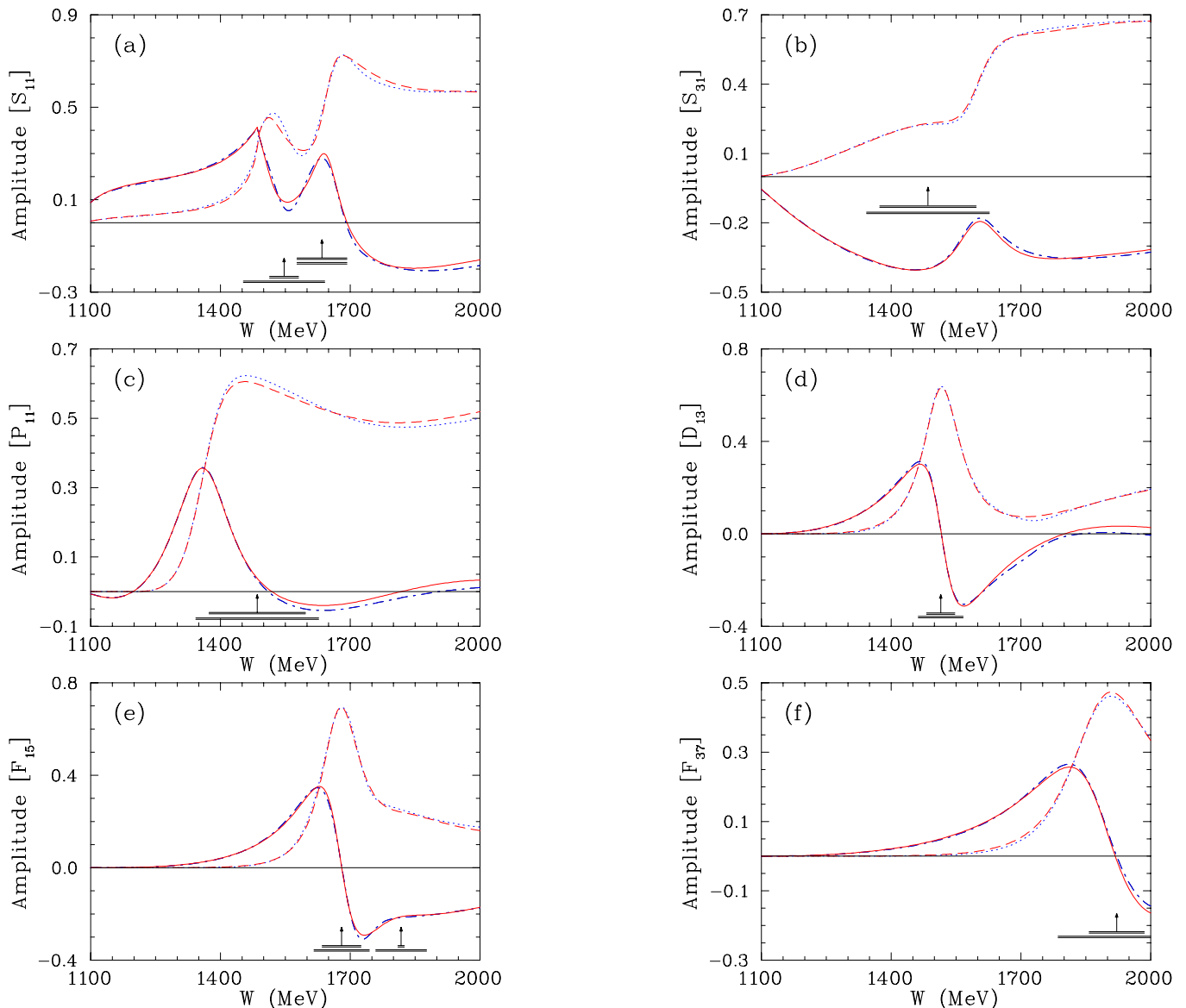


FIG. 1. (Color online) Selected partial-wave amplitudes ($L_{2l,2j}$). Solid (dashed) curves give the real (imaginary) parts of amplitudes corresponding to the WI08 [8] solution. Dash-dotted (dotted) curves give the real (imaginary) parts of amplitudes corresponding to the XP08 solution. (a) S_{11} , (b) S_{31} , (c) P_{11} , (d) D_{13} , (e) F_{15} , and (f) F_{37} . All amplitudes are dimensionless. Vertical arrows indicate Breit-Wigner resonance W_R values and horizontal bars show full Γ and partial widths for $\Gamma_{\pi N}$ associated with the GW SP06 solution [7].

Increasing the energy a small amount (10–15 MeV) to E_2 , we again diagonalize the S -matrix and evaluate the $\lambda_1(E_2), \dots, \lambda_n(E_2)$ and eigenvectors $v_1(E_2), \dots, v_n(E_2)$.

In order to track the eigenchannel, we evaluate the matrix of overlaps:

$$O_{ij}(E_1, E_2) = v_i(E_1)^\dagger v_j(E_2). \quad (9)$$

As $E_2 \rightarrow E_1$, we have

$$\lim_{E_2 \rightarrow E_1} O_{ij}(E_1, E_2) = \delta_{ij}, \quad (10)$$

which is just the statement that the eigenvectors are orthonormal. For $E_2 - E_1 \simeq 10$ MeV, we identify the

eigenvalues according to the largest overlap in the set

$$\{|O_{ij}(E_1, E_2)|\}_{j=1}^n. \quad (11)$$

Suppose, for example, that we have three channels and at the energy E_1 , we write the eigenvalues in the order:

$$\lambda_1, \lambda_2, \lambda_3. \quad (12)$$

And at energy E_2 for $i = 1$, we find that

$$|O_{13}(E_1, E_2)| > |O_{11}(E_1, E_2)| > |O_{12}(E_1, E_2)|, \quad (13)$$

then for energy E_2 , we order the eigenvalue λ_3 first; the ordering for the other eigenvalues is determined similarly.

TABLE I. Pole positions in complex energy plane of the K -matrix for the $\pi N \rightarrow \pi N$ reaction. The functional forms (see text) employed in the SAID fits are compared for selected partial waves. Each K pole position is expressed in terms of its real part.

| ℓ_{JT} | WI08 | | XP08 | |
|-------------|------|------|------|------|
| S_{11} | 1533 | 1674 | 1533 | 1702 |
| S_{31} | 1653 | | 1658 | |
| P_{11} | – | | 1517 | |
| D_{13} | – | | 1512 | 1750 |
| F_{15} | – | | 1685 | |
| F_{37} | – | | 1869 | |

IV. RESULTS

The fits with (XP08) and without (WI08) explicit CM K -matrix poles, in waves other than $(L_{2I,2J}) P_{33}$, are compared in Fig. 1. Differences in the partial waves are slight, and the fit quality is comparable over the resonance region, each fit using a similar number of parameters. This feature of the πN elastic scattering analysis seems quite stable.

In Fig. 2, we have calculated the eigenphases corresponding to the full S -matrix. Only the $\pi N \rightarrow \pi N$ and $\pi N \rightarrow \eta N$ channels have been constrained by data. We note that small changes in the partial wave T -matrix elements can result in large changes in the eigenphases. This is a corollary of the no-crossing theorem and a consequence of the non-linear nature of the diagonalization of the S -matrix. The behavior of these phases does, however, provide an interesting perspective on the emergence of resonance structures in the fits.

In the S_{11} partial wave, both fits have two eigenphases crossing 90° , at 1533 and 1674 MeV for WI08, and at 1533 and 1702 MeV for XP08. If one computes the usual Heitler K -matrix, as was done in Ref. [16], K -matrix poles are found at these energies (since the unitary transformation, U [Eq.(6)] diagonalizes K simultaneously with S and $K_{ii} = \tan \phi_i$). In the S_{31} partial wave, a 2- and 3-channel fit are compared, yielding identical crossing energies, again corresponding to a Heitler K -matrix pole (at about 1655 MeV). Note that in the WI08 plot, two eigenphase curves nearly touch, but do not cross.

In the P_{11} plot, only one of the solutions has a 90° crossing leading to a Heitler K -matrix pole. Note, however, that the energy dependence of the eigenphase crossing, and nearly crossing 90° , is very similar. This feature determines another measure of resonance behavior, to be discussed below.

The D_{13} eigenphases are quite different in the two fits. In the WI08 fit, there are no 90° crossings, while in XP08, we see two crossings. This hints at a different resonance structure, though the $\pi N T$ matrices are nearly identical.

In the F_{15} and F_{37} eigenphase plots, the XP08 solution has a single crossing, whereas the WI08 solution does not. Here also, a comparison of the eigenphases which cross, or come close to crossing, 90° have a similar energy dependence. Values of the Heitler K -matrix poles, derived

from the two solutions WI08 and XP08, for the considered partial waves, are listed in Table I.

As has been noted previously [17], resonances may be associated with a single eigenphase crossing 90° , and this will result in a Heitler K -matrix pole. However, a more robust measure (if a set of amplitudes is available) is given by the time-delay matrix [18], which is proportional to the sum of energy derivatives of all eigenphases. Other factors, such as threshold openings can also produce rapid energy dependence. Certainly the correct method of resonance identification requires the location of poles in the complex energy plane on unphysical sheets close to the physical region, which we demonstrate below. Our employment of the eigenphase approach illustrates the fact that the resonance structure may vary without significantly altering the shape of the πN elastic amplitude. It is usually the case, however, that such resonances are deep in the complex plane having large widths. Intervening zeros can also diminish the effect of poles on the physical axis.

In Fig. 3, for illustration, we plot the sum of eigenphase energy derivatives for the P_{11} and D_{13} . The peaks for P_{11} are nearly identical and occur at about 1350 MeV, which (we will see) corresponds with the real part of the pole position. For the D_{13} , peaks corresponding the PDG 4-star state, near 1500 MeV, are closely aligned. The second peak has almost no evidence in the πN elastic amplitude. However, a large contribution to the (unfitted and therefore unconstrained) $\pi\Delta$ or ρN channel produces the second peak.

In Table II, we compare the pole positions associated with resonance behavior in the plotted amplitudes. The third S_{11} pole in XP08 closely resembles the structure found in Ref. [9], at (1689, 96) MeV, by scanning all partial waves with an added Breit-Wigner contribution. The very broad (1646, 290) MeV P_{11} state is similarly close to one found in the SM90 fit [19], at (1636, 272) MeV. Two extra poles were found in the D_{13} partial wave for the XP08 solution compared to WI08. We do not intend to report the (1716, 370) MeV pole as a resonance but merely mention it here in connection with the present sensitivity study. Interestingly, the pole at (1740, 66) MeV has its effect masked by a zero intervening between the pole and real energy axis and therefore makes little impact in the physical region.

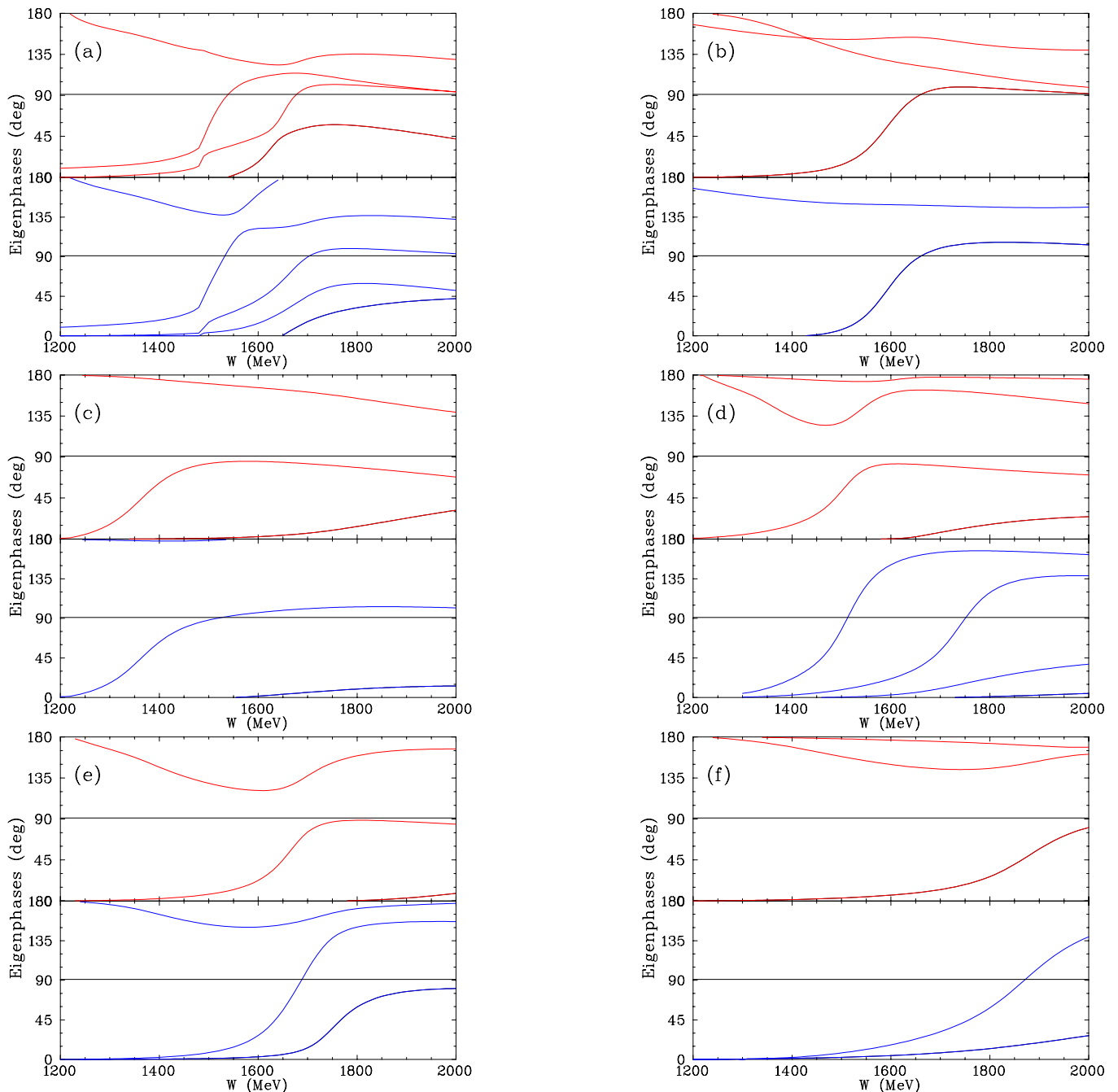


FIG. 2. (Color online) Eigenphases. (a) S_{11} , (b) S_{31} , (c) P_{11} , (d) D_{13} , (e) F_{15} , and (f) F_{37} . Upper plots correspond to WI08 solution; lower plots correspond to XP08.

As mentioned in the Introduction, a third parameterization was attempted in order to see if resonance and background contributions could be isolated using a product S -matrix approach. The form tested was $S = S_B S_R S_B$. Here S_B was constructed using the CM K -matrix method, with no pole term (polynomial only), while S_R contained only a pole (no polynomial) term. After fitting the data, the pole piece was examined but did not result in resonance parameters consistent with previous determinations. In hindsight, this could have been

anticipated, as the polynomial form of the CM K -matrix is capable of generating T -matrix poles, and therefore is not really a “background” in this approach.

V. CONCLUSIONS

We have reported an extensive study of the parameterization dependence of our πN elastic amplitudes and resonance spectrum, using very different forms for the

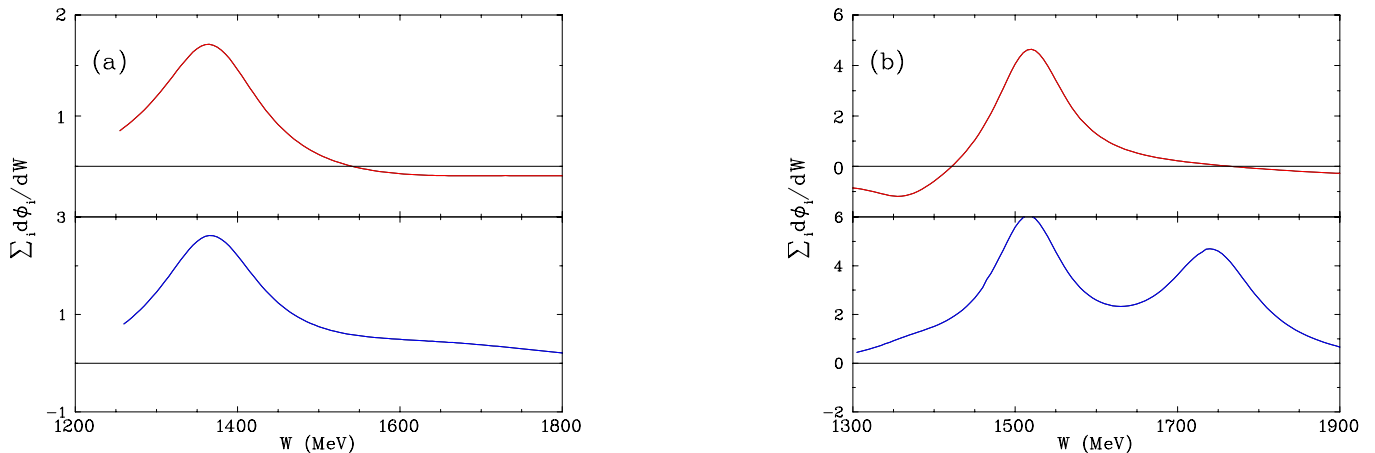


FIG. 3. (Color online) Derivatives of eigenphases. (a) P_{11} and (b) D_{13} . Upper plots correspond to WI08 solution; lower plots correspond to XP08.

TABLE II. Pole positions in complex energy plane of the T -matrix for the $\pi N \rightarrow \pi N$ reaction. The functional forms (see text) employed in the SAID fits are compared for selected partial waves. Each T pole position is expressed in terms of its real and imaginary parts ($M_R, -\Gamma_R/2$) in MeV. The second sheet pole is labeled by a †.

| ℓ_{JT} | WI08 | | | XP08 | | |
|-------------|-------------|-------------|-------------|-------------|-------------|-------------|
| S_{11} | (1499, 49) | (1647, 42) | (1666, 260) | (1538, 65) | (1675, 58) | (1690, 121) |
| S_{31} | (1594, 68) | | | (1592, 66) | | |
| P_{11} | (1358, 80) | (1388, 82)† | | (1358, 80) | (1387, 80)† | (1646, 290) |
| D_{13} | (1515, 55) | | | (1513, 53) | (1740, 66) | (1716, 370) |
| F_{15} | (1674, 57) | (1779, 138) | | (1672, 70) | (1734, 61) | |
| F_{37} | (1883, 115) | | | (1874, 119) | | |

CM K -matrix, with explicit poles in each partial wave. The partial-wave amplitudes were found to be very stable under this change.

The eigenphase representation was introduced as it gives an interesting visualization of both T -matrix and Heitler K -matrix poles in a single figure, and because it provides a more concrete example of properties discussed in older works. This discussion also provides a continuation of the study started in Ref. [16].

The more formally correct extraction of pole positions has revealed structures mainly found in earlier fits to the πN elastic scattering data. As the partial wave amplitudes have not changed significantly, the effects of new resonances must be minimized through large widths, intervening zeros, or small coupling to the πN channel. The added CM K -matrix poles have in most cases become the generators of the dominant T -matrix poles, previously generated via the polynomial form, rather than producing further resonances. This could be determined by turning off either the CM K -matrix pole or polynomial terms and seeing the effect on the extracted T -matrix poles.

In the SM90 fit, a study of the resonance spectrum was tried where, in addition to experimental data, the amplitudes from the KH [5] and CMB [6] analyses were added as soft constraints. A possible extension to the present

work would be a re-examination of the resonance spectrum from a fit, with explicit CM K -matrix poles, constrained to more closely follow either the KH and CMB PWA results, or a multi-channel analysis.

ACKNOWLEDGMENTS

This work was supported in part by the U.S. Department of Energy Grant DE-FG02-99ER41110.

-
- [1] J. Beringer, *et al.* (Particle Data Group), Phys. Rev. D **86**, 010001 (2012).
- [2] P. Morsch, Int. J. Mod. Phys. A **20**, 1699 (2005).
- [3] M. Ablikim, *et al.*, Phys. Rev. Lett. **97**, 06201 (2006).
- [4] For a review, see E. Klempt and J. M. Richard, Rev. Mod. Phys. **82**, 1095 (2010).
- [5] G. Höhler, *Pion-Nucleon Scattering*, ed. H. Schopper, Vol. I/9b2 (Landolt-Börnstein, Springer Verlag, 1983).
- [6] R. E. Cutkosky, *et al.*, *IV International Conference on Baryon Resonances (Baryon 1980)*, Toronto, ed. N. Isgur, p. 19.
- [7] R. A. Arndt, W.J. Briscoe, I.I. Strakovsky, and R.L. Workman, Phys. Rev. C **74**, 045205 (2006).
- [8] A selection of fits and the full database are available at: <http://gwdac.phys.gwu.edu>.
- [9] R. A. Arndt, I. I. Strakovsky, R. L. Workman, and M. M. Pavan, Phys. Rev. C **52**, 2120 (1995).
- [10] R. A. Arndt, J. M. Ford, and L. D. Roper, Phys. Rev. D **32**, 1085 (1985).
- [11] R. A. Arndt, W. J. Briscoe, I. I. Strakovsky, R. L. Workman, and M. M. Pavan, Phys. Rev. C **69**, 035213 (2004).
- [12] M. W. Paris and R. L. Workman, Phys. Rev. C **82**, 035202 (2010).
- [13] J.-L. Basdevant and E. L. Berger, Phys. Rev. D **19**, 239 (1979).
- [14] W. Zimmerman, Nuovo Cim. **21**, 249 (1961).
- [15] E. P. Wigner and J. von Neumann, Z. Phys. **30**, 467 (1929).
- [16] R. L. Workman, R. A. Arndt, and M. W. Paris, Phys. Rev. C **79**, 038201 (2009).
- [17] S. Ceci, *et al.*, Phys. Lett. B **659**, 228 (2008).
- [18] R. H. Dalitz and R. G. Moorhouse, Proc. Roy. Soc. Lond. **318**, 279 (1970); F. T. Smith, Phys. Rev. **118**, 349 (1960).
- [19] R. A. Arndt, Z. Li, L. D. Roper, R. L. Workman, and J. M. Ford, Phys. Rev. D **43**, 2131 (1991).